Terpenoids with a New Skeleton and Novel Triterpenoids with Anti-inflammatory Effects from *Garcinia subelliptica*

Jing-Ru Weng,[a] Chun-Nan Lin,*[a] Lo-Ti Tsao,[b] and Jih-Pyang Wang[b]

Abstract: Three novel phloroglucinol derivatives, garcinielliptones F (**1**), H (**3**), and I (**4**), and two novel terpenoids, garcinielliptones G (**2**) and J (**5**), with a new skeleton have been isolated from the seeds of *Garcinia subelliptic*a. Their structures, including relative configurations, were elucidated by spectroscopic methods and computer-generated molecular modeling. Compound **1** showed potent inhibitory effects on the release of β-glucuronidase and lysozyme from rat neutrophils that had been stimulated with formyl-Met-Leu-Phe (fMLP)/cytochalasin B (CB). This effect was concentration-dependent with IC_{50} values of 26.9 ± 2.6 and 20.0 ± 1.3 μM, respectively. Compound **1** also showed a potent concentration-dependent inhibitory effect on superoxide anion generation in rat neutrophils stimulated with fMLP/CB, with an IC_{50} value of 17.0 ± 0.9 μM. Compound **4** showed a potent inhibitory effect on NO production in culture media of N9 cells in response to lipopolysaccharide (LPS)/interferon-γ (IFN-γ) in a concentration-dependent manner with an IC_{50} value of 7.4 ± 0.2 μM.

Keywords: anti-inflammatory activity · drug design · *Garcinia subelliptica* · phloroglucinol derivatives · terpenoids

Introduction

Various constituents and antioxidant xanthones from the wood and root bark of *Garcinia subelliptica* Merr. (Guttiferae) have been reported.[1,2] In the search for bioactive constituents in Formosan Guttiferae plants, the bioactive constituents of the seeds of *G. subelliptica* were investigated, and three novel triterpenoids and four novel phloroglucinol derivatives, have been reported.[3–5] A further study investigating the constituents of the seeds of *G. subelliptica* yielded three novel phloroglucinol derivatives, garcinielliptones F (**1**) , H (**3**), and I (**4**), and two novel terpenoids, garcinielliptones G (**2**) and J (**5**), with a new skeleton. Garsubellin A and garcinielliptin oxide, isolated from the seeds of this plant, strongly inhibited the chemical-mediator release from mast cells and neutrophils.[5] The structure elucidation of the five novel compounds and the anti-inflammatory effects are reported.

Results and Discussion

The molecular formula of **1** (Figure 1) was proposed as $C_{30}H_{44}O_5$ by chemical ionization mass spectrometry (CIMS) (*m/z*: 483 $[M-H]^-$), which was consistent with the ^1H and ^{13}C NMR data. The IR spectrum (film on NaCl) showed carbonyl (1724 cm^{-1}), conjugated carbonyl (1639 cm^{-1}), and OH (3439 cm^{-1}) functionalities. The ^1H NMR spectrum of **1** (Table 1) resembled that of garsubellin D (**6**),[6] except for the absence of signals due to a 2β-hydroxyisopropyl-2,3-dihydrofuran ring and the appearance of signals due to a 3-hydroxy-3-methylbut-1-enyl group. The heteronuclear multiple-bond correlation (HMBC) correlations of H-17/C-3 and C-5, and H-18/C-4 established the connectivities between C-3 and C-4, C-4 and C-5, C-4 and C-17, and C-17 and C-18.

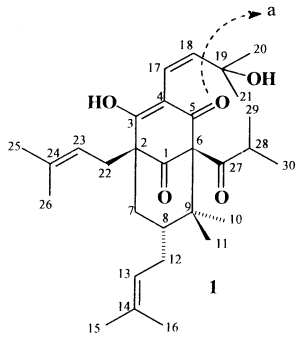

Figure 1. Structure and MS fragmentation pattern of **1**.

[a] Prof. C.-N. Lin, J.-R. Weng
School of Pharmacy, Kaohsiung Medical University
Kaohsiung, Taiwan 807 (R. China)
Fax: (+886) 7-5562365
E-mail: lincna@cc.kmu.edu.tw

[b] L.-T. Tsao, Prof. J.-P. Wang
Department of Education and Research
Taichung Veterans General Hospital
Taichung, Taiwan 407 (R. China)

DOI: 10.1002/chem.200305209

Table 1. ^{1}H and ^{13}C NMR data of **1** and **2** in $CDCl_3$. Arbitrary numbering see Figures 1 and 3; δ in ppm, J in Hz.

	1			**2**		
	δH	δC	HMBC	δH	δC	HMBC
1		206.3	1.39 (H_α-7), 2.41 (H_α-22), 2.49 (H_β-22)		205.7	2.53 (H_β-6)
2		56.7	1.39 (H_α-7), 1.89 (H_β-7), 2.41 (H_α-22), 2.49 (H_β-22)		61.0	2.53 (H_β-6)
3		170.8	1.39 (H_α-7), 1.89 (H_β-7), 6.47 (H-17)		90.2	1.34 (H_α-6), 6.01 (H-17)
4		114.5	5.34 (H-18)		209.1	
5		188.3	6.47 (H-17)		82.8	1.11 (Me-9), 1.17 (Me-10)
6		83.5	1.00 (Me-10), 1.22 (Me-11)	α1.34 (m) β2.53 (m)	40.2	1.60 (H_α-22)
7	α1.39 (m) β1.89 (dd, 13.2, 3.2)	39.2	2.09 (H_β-12)	1.65 (m)	43.1	1.11 (Me-9), 1.17 (Me-10)
8	1.44 (m)	43.3	1.00 (Me-10), 1.22 (Me-11), 1.39 (H_α-7), 1.89 (H_β-7)		55.8	1.11 (Me-9), 1.17 (Me-10), 2.53 (H_β-6)
9		46.8	1.00 (Me-10), 1.22 (Me-11), 1.89 (H_β-7)	1.11 (s)	17.3	
10	1.00 (s)	21.5	1.22 (Me-11)	1.17 (s)	21.3	
11	1.22 (s)	22.9	1.00 (Me-10)	α2.13 (dd, 13.2, 8.0) β2.50 (m)	27.9	
12	α1.67 (m) β2.09 (m)	26.5	4.95 (H-13)	5.14 (t, 6.4)	118.6	1.46 (Me-15), 1.62 (Me-14), 2.50 (H_β-11)
13	4.95 (t, 7.2)	122.6	2.09 (H_β-12)		133.5	1.46 (Me-15), 1.62 (Me-14), 2.50 (H_β-11)
14		133.8	1.64 (Me-15), 1.65 (Me-16), 1.67 (H_α-12)	1.62 (s)	25.9	1.46 (Me-15)
15	1.64 (s)	25.9	4.95 (H-13)	1.46 (s)	17.7	1.62 (Me-14)
16	1.65 (s)	25.7	4.95 (H-13)		192.4	6.97 (H-18)
17	6.47 (d, 10.0)	115.4	5.34 (H-18)	6.01 (d, 10.8)	122.8	
18	5.34 (d, 10.0)	123.7	1.43 (Me-21)	6.97 (d, 10.8)	156.2	
19		81.9	1.39 (Me-20), 1.43 (Me-21), 5.34 (H-18), 6.47 (H-17)		74.1	1.44 (Me-20), 1.67 (Me-21), 6.01 (H-17), 6.97 (H-18)
20	1.39 (s)	28.6		1.44 (s)	30.0	1.67 (Me-21)
21	1.43 (s)	28.3	5.34 (H-18)	1.67 (s)	29.9	1.44 (Me-20)
22	α2.41 (dd, 14.8, 8.0) β2.49 (dd, 14.8, 6.0)	29.0		α1.60 (m) β2.05 (dd, 13.2, 8.0)	27.4	5.04 (H-23)
23	5.00 (t, 7.2)	119.3	2.41 (H_α-22), 2.49 (H_β-22)	5.04 (t, 6.4)	122.5	1.58 (Me-25), 1.71 (Me-26)
24		133.3	2.41 (H_α-22), 2.49 (H_β-22)		133.0	1.58 (Me-25), 1.71 (Me-26)
25	1.54 (s)	17.8	5.00 (H-23)	1.58 (s)	17.8	
26	1.67 (s)	18.1	5.00 (H-23)	1.71 (s)	25.7	1.58 (Me-25)
27		209.0	1.02 (Me-30), 1.11 (Me-29)		206.5	0.90 (Me-29), 1.01 (Me-30)
28	2.07 (m)	42.5	1.02 (Me-30), 1.11 (Me-29)	2.50 (m)	39.7	0.90 (Me-29), 1.01 (Me-30)
29	1.11 (d, 6.4)	20.5		0.90 (d, 6.8)	19.6	
30	1.02 (d, 6.4)	15.6		1.01 (d, 6.8)	19.7	

The $^{1}H,^{1}H$ COSY correlation of H-17/H-18 and the HMBC correlations of H-17/C-19, H-18/C-19 and C-4, Me-20/C-19, and Me-21/C-19 confirmed that the 3-hydroxy-3-methylbut-1-enyl group was linked at C-4. In the ^{13}C NMR spectrum of **1** (Table 1), the chemical shift values of **1** were almost identical to the corresponding data of **6**, except for C-3, C-4, and C-17–C-21. Thus, garcinielliptone F (**1**) was characterized as having a bicyclo[3.3.1]nonane moiety. The presence of characteristic peaks at $m/z = 482$ $[M-2H]^-$, 466 $[M-H_2O]^-$, and 424 $[M-a-H]^-$ ($a \equiv C_3H_7O$, see Figure 1) in its CIMS also supported the characterization of **1**.[7]

Abstract in Chinese :

由福木種子分離得到三個新穎的 phloroglucinol 衍生物，garcinielliptones F (**1**)，H (**3**)與 I (**4**)及二個具有新骨架的新穎三帖類，garcinielliptones G (**2**)與 J (**5**)。化學結構及相對立體係由測定光譜方法證明。化合物 **1** 對老鼠嗜中性白血球以 formyl-Met-Leu-Phe (fMLP)/cytochalasin B (CB)引發之β–glucuronidase 及溶小體酶釋放，其抑制活性呈現與濃度有關的現象，IC_{50} 值分別為 26.9 ± 2.6 及 20.0 ± 1.3 μM。化合物 **1** 亦對老鼠嗜中性白血球以 fMLP/CB 引發過氧陰離子的形成，也呈現抑制活性與濃度有關的現象，且 IC_{50} 值為 17.0 ± 0.9 μM。化合物 **4** 對細胞培養皿中的 N9 cells 以 lipopolysaccharide (LPS)/interferon-γ (IFN-γ)引發之一氧化氮形成，其抑制活性呈現與濃度有關的現象，IC_{50} 值為 7.4 ± 0.2 μM。

The relative configurations at C-2, C-6, and C-8 were determined by comparison with the relative stereochemistry of **6**. NOESY experiment on **1** showed cross peaks between H_β-7/H_2-22, H_β-7/H-8, Me-16/Me-10, and Me-11/H-28; this suggests that the prenyl groups at C-2 and C-8, and the 1-oxo-2-methylpropyl group at C-6 are on the β, α, and β sides of **1**, respectively.

From the ^{1}H NMR, COSY, and NOESY spectra, a computer-generated 3D structure was obtained by using the molecular modeling program CS CHEM 3D V 3.5.1, with MM2 force-field calculations for energy minimization (Figure 2). The calculated distances between H_β-7/H_2-22 (2.554 Å), H_β-7/H-8 (2.271 Å), Me-16/Me-10 (2.832 Å), and Me-11/H-28 (2.111 Å) are all less than 4.00 Å; this is consistent with the well-defined NOESY observed for each of these proton pairs. Thus, garcinielliptone F (**1**) was characterized as 9,9-dimethyl-2,8-di(γ,γ-dimethylallyl)-3-hydroxy-4-(3-hydroxy-3-methylbut-1-enyl)-6-(1-oxo-2-methylpropyl)-8β-*H-cis*-bicyclo[3.3.1]non-3-en-1,5-dione (**1**).

The molecular formula of **2** was determined as $C_{30}H_{44}O_6$ by high-resolution electron-impact mass spectrometry (HR-EIMS) (m/z: 498.2996 $[M-2]^+$); this was consistent with the ^{1}H and ^{13}C NMR data.[7] The IR spectrum (film on NaCl)

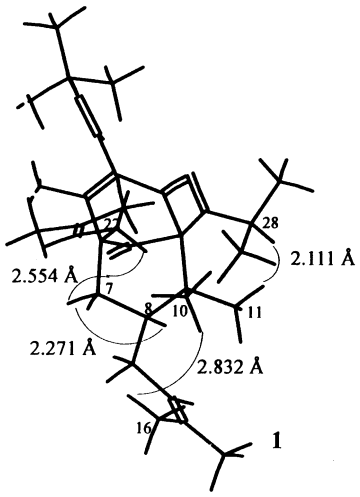

Figure 2. Selected NOESY correlations and relative configuration of **1**.

showed carbonyl (1767, 1727, 1708 cm^{-1}), a conjugated carbonyl (1665 cm^{-1}), and OH (3454 cm^{-1}) functionalities. The ^1H NMR spectrum of **2** (Table 1) revealed the proton signals of two γ,γ-dimethylallyl units, two secondary methyl, four tertiary methyl, a methylene, two methine, and two olefinic groups. The ^{13}C NMR spectrum of **2** showed the presence of ten methyls, three methylenes, two methines, four olefinic carbons, and eleven quaternary carbons, including two oxygenated carbons and four carbonyl carbons. The $^1H,^1H$ COSY correlations of H_2-6/H-7, H-7/H_β-11, H_α-11/H-12, H-17/H-18, H_2-22/H-23, and H-28/Me-29 and Me-30 established the partial moieties represented with bold lines in **2** (Figure 3). The HMBC correlations of H_2-22/C-6, H_β-6/C-1 and C-2, H_α-6/C-3 established the connectivities between C-22 and C-2, C-1 and C-2, C-2 and C-3, and C-2 and C-6. The HMBC correlations of H-17/C-19, H-18/C-16 and C-19, Me-20/C-18 and C-21, and Me-21/C-18 and C-19 established the 4-hydroxy-4-methyl-1-oxopent-2-enyl group, and the HMBC correlation of H-17/C-3, an oxygenated quaternary carbon, confirmed the connectivity between C-3 and C-16 and a hydroxy group located at C-3. The HMBC correlations of C-8/H_β-6, Me-9, and Me-10, C-5/Me-9 and Me-10, C-7/Me-9 and Me-10 established that C-7 was linked through C-8 to C-5, and that Me-9 and Me-10 were located at C-8. The HMBC correlations of C-12/Me-14 and Me-15, H-12/C-14 and C-15, C-13/H_β-11 and Me-15, Me-15/C-14, and Me-14/C-15 confirmed the second prenyl group was linked to C-7. The HMBC correlations of C-27/H-28, Me-29, and Me-30 confirmed the connectivity between C-27 and C-28. Based on the above results, and that C-4 and C-5 are quaternary carbon atoms, the connectivity between C-4 and C-5, and C-5 and C-27 was established. Thus, garcinielliptone G was characterized as **2** with a new bicyclo[3.2.1]octane moiety. The EIMS of **2** did not show a molecular ion but indicated significant peaks at $m/z = 498$ $[M-2]^+$, 482 $[M-H_2O]^+$, 414 $[M-a-H]^+$, and 343 $[M-a-b-H_2O+H]^+$ ($a \equiv C_5H_9O$, $b \equiv C_4H_7$ see Figure 3), which also supported the characterization of **2**.

The NOESY experiment of **2** showed selected cross peaks as shown in the 3D drawing (Figure 4). The relative configurations at C-2, C-3, C-5, and C-7 were deduced from the NOESY cross peaks of Me-25/H_α-6, H_α-6/Me-14, H_β-6/H-7, H_α-11/Me-10, Me-10/Me-21, and Me-10/Me-29. Consequently, the prenyl groups at C-2 and C-7, the 1-oxo-2-methylpropyl group at C-5, and the 4-hydroxy-4-methyl-1-oxo-2-pentenyl group at C-3 are on the α side of **2**.

Based on the information from the ^1H NMR, COSY, and NOESY spectra, a computer-generated 3D structure was obtained by using the above-mentioned molecular modeling program with MM2 force-field calculations for energy minimization. The calculated distances between Me-25/H_α-6 (2.537 Å), H_α-6/Me-14 (2.542 Å), H_β-6/H-7 (2.540 Å), H_α-11/Me-10 (3.150 Å), Me-10/Me-21 (3.878 Å), and Me-10/Me-29 (2.801 Å) are all less than 4.00 Å; this is consistent with the well-defined NOESY observed for each of the proton pairs. Thus, garcinielliptone G (**2**) was characterized as 8,8-dimethyl-2,7β-*H*-di(γ,γ-dimethylallyl)-3β-hydroxy-3-(1-oxo-4-hydroxy-4-methylpent-2-enyl)-5-(1-oxo-2-methylpropyl)-*cis*-bicyclo[3.2.1]octa-1,4-dione.

The molecular formula of **3** was determined as $C_{30}H_{48}O_8$ by HR-EIMS (m/z: 518.3251 $[M-H_2O]^+$); this was consistent with the ^1H and ^{13}C NMR data. The IR spectrum (film on NaCl) showed carbonyl (1731, 1712, and 1694 cm^{-1}), and OH (3439 cm^{-1}) functionalities. The ^1H NMR spectrum of **3** (Table 2) revealed the proton signals of one γ,γ-dimethylallyl, two secondary methyl, six tertiary methyl, four methylene, an oxymethine, and two methine groups. The ^{13}C NMR spectrum of **3** showed the presence of ten methyls, five methylenes, two methines, an oxygenated tertiary carbon, an

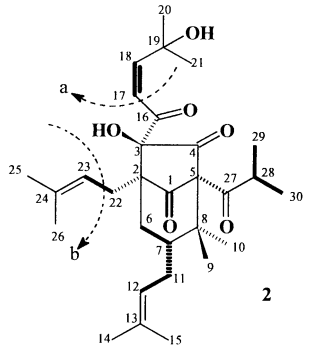

Figure 3. Structure, substructure (bold lines), and MS fragmentation pattern of **2**.

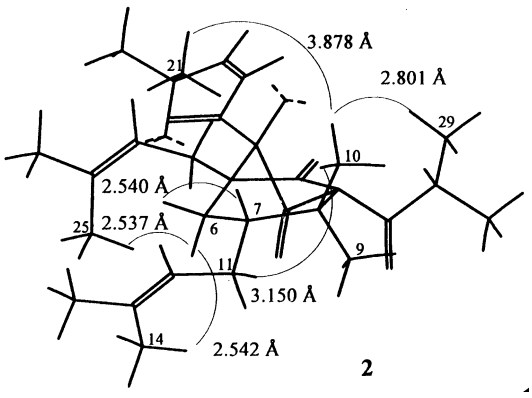

Figure 4. Selected NOESY correlations and relative configuration of **2**.

Table 2. ^{1}H and ^{13}C NMR data of **3** and **5** in $CDCl_3$. Arbitrary numbering see Figures 5 and 9; δ in ppm, J in Hz.

	3			**5**		
	δH	δC	HMBC	δH	δC	HMBC
1		203.4	1.89 (H_α-22), 2.29 (H_β-22), 4.45 (OH-2)		172.0	1.50 (H_α-5), 2.36 (H_α-15)
2	2-OH (4.45)	74.2	1.89 (H_α-22), 2.29 (H_β-22), 4.45 (OH-2)		56.8	2.12 (H_β-5), 2.36 (H_α-15)
3		104.0	1.28 (H_α-7), 2.29 (H_β-22), 2.44 (H_β-7), 2.88 (H_β-17)		201.4	2.12 (H_β-5), 2.36 (H_α-15)
4		61.9	1.28 (H_α-7), 1.48 (H_α-17), 2.44 (H_β-7), 2.88 (H_β-17)		97.0	1.07 (Me-9), 1.13 (Me-8)
5		204.7	2.44 (H_β-7), 2.88 (H_β-17)	α1.50 (d, 12.8) β2.12 (dd, 12.8, 4.4)	41.0	
6		80.1	1.00 (Me-10), 1.34 (Me-11)	1.62 (m)	41.7	1.07 (Me-9), 1.13 (Me-8), 1.50 (H_α-5)
7	α1.28 (m) β2.44 (dd, 13.6, 3.6)	39.3	2.06 (H_β-12)		49.2	1.07 (Me-9), 2.12 (H_β-5)
8	1.53 (m)	42.9	1.00 (Me-10), 1.34 (Me-11), 1.48 (H_α-12), 2.44 (H_β-7)	1.13 (s)	16.0	1.07 (Me-9)
9		51.4	1.00 (Me-10), 1.34 (Me-11)	1.07 (s)	22.4	1.13 (Me-8)
10	1.00 (s)	17.9		α1.68 (m) β2.02 (dd, 10.4, 6.0)	27.4	
11	1.34 (s)	26.3		4.99 (t, 6.4)	121.5	1.55 (Me-13), 1.68 (Me-14)
12	α1.48 (m) β2.06 (dd, 13.6, 6.0)	27.6	5.02 (H-13)		134.1	1.55 (Me-13), 1.68 (Me-14)
13	5.02 (t, 6.4)	122.9	1.53 (Me-15), 1.63 (Me-16)	1.55 (s)	17.8	1.68 (Me-14)
14		132.3	1.53 (Me-15), 1.63 (Me-16), 2.06 (H_β-12)	1.68 (s)	25.8	1.55 (Me-13)
15	1.53 (s)	17.7		α2.36 (dd, 14.8, 7.6) β2.42 (dd, 14.8, 7.6)	26.2	
16	1.63 (s)	25.7		5.04 (t, 6.4)	116.9	1.62 (Me-19), 2.42 (H_β-15)
17	α1.48 (m) β2.88 (dd, 13.6, 8.0)	32.6			136.5	1.62 (Me-19), 2.42 (H_β-15)
18	4.04 (t, 8.0)	82.6	2.88 (H_β-17)	1.67 (s)	18.0	
19		71.5	1.18 (Me-21), 1.24 (Me-20), 2.88 (H_β-17), 4.04 (H-18)	1.62 (s)	25.7	
20	1.24 (s)	26.2			205.1	0.90 (Me-23), 1.05 (Me-22)
21	1.18 (s)	31.2		3.00 (m)	37.9	0.90 (Me-23), 1.05 (Me-22)
22	α1.89 (m) β2.29 (m)	24.8		1.05 (d, 6.8)	17.0	0.90 (Me-23)
23	α1.61 (m) β1.80 (m)	33.4	1.89 (H_α-22)	0.90 (d, 6.8)	17.9	1.05 (Me-22)
24		74.8	1.18 (Me-26), 1.32 (Me-25), 1.89 (H_α-22), 2.29 (H_β-22)			
25	1.32 (s)	24.0				
26	1.18 (s)	26.2				
27		208.3				
28	3.02 (m)	39.5				
29	0.97 (d, 6.4)	19.5				
30	0.88 (d, 6.4)	20.5				

olefinic carbon, and eleven quaternary carbons, including four oxygenated and three carbonyl carbons. The $^{1}H,^{1}H$ COSY correlations of H-12/H-13, H-8/H-12, H_2-17/H-18, H_2-22/H-23, and H-28/Me-29 and Me-30, established the partial moieties represented as bold lines in **3** (Figure 5). The HMBC correlations of H_2-22/C-1 and C-2, and H_β-22/C-3 established the connectivities between C-1 and C-2, C-2 and C-3, and C-2 and C-22, and the HMBC correlations of H_2-22/C-24 and C-24/Me-25 and Me-26 confirmed that the 3-hydroxy-3-methylbutyl group was linked at C-2. The HMBC correlations of H_β-17/C-3, C-4, C-5 and C-19, and C-19/Me-20 and Me-21 established the 3,4-dihydropyran moiety and the connectivity between C-4 and C-5. The above results also indicated that the pyran ring should be fused between C-3 and C-4. The HMBC correlations of H_2-7/C-4, H_β-7/C-5, C-8, and C-9, and H_α-7/C-9, confirmed the connectivities between C-7 and C-8, and C-8 and C-9. The HMBC correlations of C-13/Me-15 and Me-16, C-14/Me-15, Me-16, and H_β-12 and H_β-12/C-7 confirmed that the prenyl group was linked at C-8. The HMBC correlations of Me-10/C-8 and C-9, and Me-11/C-8 and C-9 confirmed that the Me-10 and Me-11 were linked together at C-9 and the connectivity between C-8 and C-9. The HMBC correlations of C-27/Me-29 and Me-30, and C-6/Me-10 and Me-11, the NOESY correlation of Me-26/Me-29, and that C-5 and C-6 both present as quaternary carbons, established the connectivities between C-5 and C-6, C-6 and C-9, and that the 1-oxo-2-methylpropyl group was linked at C-6. The IR band

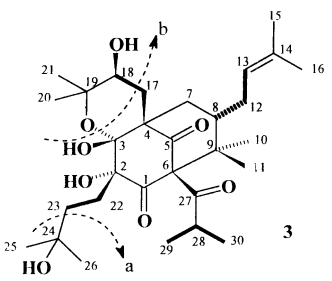

Figure 5. Structure, substructure (bold lines), and MS fragmentation pattern of **3**.

and ^{13}C NMR spectra (Table 2) showed the presence of two quaternary hydroxy groups at C-2 and C-3. The presence of significant peaks at $m/z = 518$ $[M-H_2O]^+$, 461 $[518-a+2H]^+$, 448 $[518-Me-55]^+$, and 430 $[518-b]^+$ ($a \equiv C_3H_7O$, $b \equiv C_4H_8O_2$, see Figure 5) in the EIMS also supported the characterization of **3**. Thus, garcinielliptone H (**3**) was characterized as having a new 3β-hydroxy-3,4-dihydro-2*H*-pyrano[3,2-*b*]bicyclo[3.3.1]nonane skeleton.

The NOESY experiment of **3** showed selected cross peaks as shown in the 3D drawing (Figure 6). The relative configurations at C-2, C-3, C-4, C-6, C-8, and C-18 were deduced from the NOESY cross peaks of H_β-7/H-8, H-8/-Me-11, Me-11/Me-30, Me-29/Me-26, H_α-7/H_α-17, H_α-17/H-18, H-18/Me-20, and H-18/Me-21, while the 3-hydroxy-3-methylbutyl group at C-2, the hydroxy groups at C-3 and C-18, the 1-oxo-2-methylpropyl group at C-6, and the bond between C-4 and C-17 are on the β side, and the hydroxy group at C-2, C-3-O of 3-hydroxy-2,2-dimethyl-3,4-dihydropyran moiety on the C-3–C-4 bond, and the prenyl group at C-8 are on the α side of **3**.

Based on the information from the ^1H NMR, COSY, and NOESY spectra, a computer-generated 3D structure was obtained by using the above-mentioned molecular modeling program with MM2 force-field calculations for energy minimization. The calculated distances between H_β-7/H-8 (2.293 Å), H-8/Me-11 (2.285 Å), Me-11/Me-30 (2.255 Å), Me-29/Me-26 (2.659 Å), H_α-7/H_α-17 (3.596 Å), H_α-17/H-18 (2.628 Å), H-18/Me-20 (2.346 Å), and H-18/Me-21 (3.697 Å) are all less than 4.00 Å; this is consistent with the well-defined NOESY observed for each of the proton pairs. Thus, garcinielliptone H (**3**) was characterized as 2α,3β-dihydroxy-9,9-dimethyl-3,4-(2,2-dimethyl-3β-hydroxy-3,4-dihydro-2*H*-pyran)-8-(γ,γ-dimethylallyl)-2-(3-hydroxy-3-methylbutyl)-6-(1-oxo-2-methylpropyl)-8β-*H-cis*-bicyclo[3.3.1]nona-1,5-dione.

The molecular formula of **4** was determined as $C_{33}H_{42}O_5$ by HR-EIMS (m/z: 518.3036 $[M]^+$), which was consistent with the ^1H and ^{13}C NMR data. The IR spectrum (film on NaCl) showed carbonyl (1720 cm^{-1}), conjugated carbonyl (1694 cm^{-1}), aromatic ring (1620 cm^{-1}), and OH (3470 cm^{-1}) functionalities. The ^1H and ^{13}C NMR spectra of **4** (see Experimental Section) resembled those of hyperibone B[8] but showed different optical rotation.[8] Thus, the structure of garcinielliptone I (**4**) was assigned as the stereoisomer of hyperibone B (Figure 7).

The NOESY experiment of **4** showed selected cross peaks as shown in the 3D drawing (Figure 8). The relative configurations at C-2, C-6, C-8, and C-18 were deduced from NOESY cross peaks of H_2-22/H_α-7, H_β-7/H-8, Me-16/Me-10, and H-18/H_α-17, and H-32 or H-30/Me-10. The prenyl groups at C-2 and C-8, and benzoyl group at C-6 are on the α side of **4**, while the 2β-hydroxyisopropyl group at C-18 is on the β side of the molecule.

Based on the information from the ^1H NMR, COSY, and NOESY spectra, a computer-generated 3D structure was obtained by using the above-mentioned molecular modeling program with MM2 force-field calculations for energy minimization. The calculated distances between H_2-22/H_α-7 (2.591 Å), H_β-7/H-8 (2.450 Å), Me-16/Me-10 (3.353 Å), H-18/H_α-17 (2.332 Å), and H-32 or H-30/Me-10 (3.707 Å) are all less than 4.00 Å; this is consistent with the well-defined NOESY spectra observed for each of the proton pairs. Thus, garcinielliptone I (**4**) was characterized as 6-benzoyl-9,9-dimethyl-2,8-di(γ,γ-dimethylallyl)-3,4-(2β-hydroxyisopropyldihydrofuran)-8β-*H-cis*-bicyclo[3.3.1]nona-3-en-1,5-dione (**4**).

The molecular formula of **5** was determined as $C_{23}H_{34}O_4$ by HR-EIMS (m/z: 374.2459 $[M]^+$), which was consistent with the ^1H and ^{13}C NMR data. The IR spectrum (film on NaCl) showed a γ-lactone ring (1801 cm^{-1}) and carbonyl

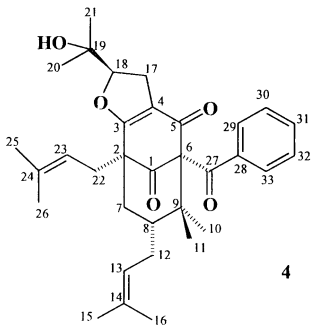

Figure 7. Structure of **4**.

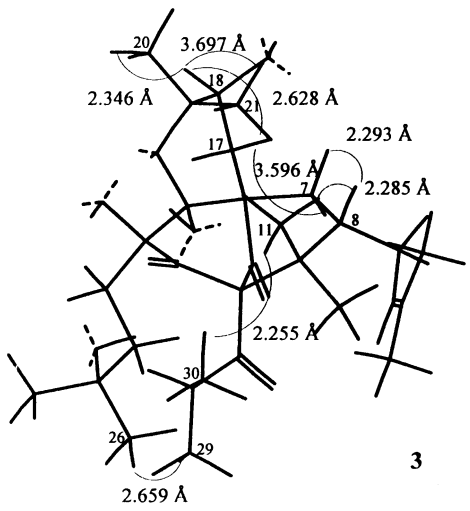

Figure 6. Selected NOESY correlations and relative configuration of **3**.

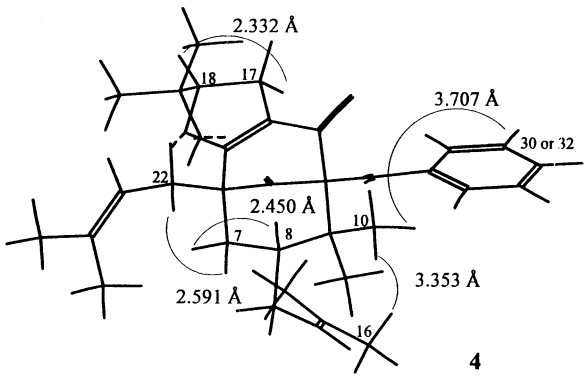

Figure 8. Selected NOESY correlations and relative configuration of **4**.

(1764, 1712 cm^{-1}) functionalities.[9] The ^1H NMR spectrum of **5** (Table 2) revealed the proton signals of two γ,γ-dimethylallyl, two secondary methyl, two tertiary methyl, one methylene, and two methine groups. The ^{13}C NMR spectrum of **5** showed the presence of eight methyls, three methylenes, four methines, and eight quaternary carbons, including two carbonyl carbons and a γ-lactonic carbon. The $^1H,^1H$ NMR connectivity experiments (COSY, LRCOSY) and the $^1H,^{13}C$ NMR connectivity experiments (HMQC, HMBC) clearly established the substructures **a–c** depicted as boldface in Figure 9.

The HMBC correlations of H_α-15/C-1, C-2, and C-3 established the connectivities between C-15 and C-2, C-1, and C-2, and between C-2 and C-3, while the NOESY cross peak of H_β-5/H_β-15 confirmed that substructure **b** was linked at C-2. The HMBC correlations of H_α-5/C-6, H_β-5/-C-2, C-3, and C-7, Me-8/C-4, C-6, and C-9, Me-9/C-4, C-7, C-6, and C-8 established the connectivities between C-2 and C-5, C-5 and C-6, C-6 and C-7, C-7 and C-8, and C-7 and C-9. The $^1H,^1H$ COSY correlation of H-6/H_2-10, the NOESY correlations of Me-8/H_β-10, Me-23/Me-8, and the fact that C-3 and C-4 are present as quaternary carbons, confirmed that substructures **a** and **c** were linked at C-4 and C-6, respectively, and established the connectivity between C-3 and C-4. Thus, garcinielliptone J (**5**) was characterized as having a novel 1,2,3,4-tetrahydrofurano[1,4-*af*]cyclohexa-1,3-dione moiety. The presence of significant peaks at $m/z = 306$ $[M-Me-d+2H]^+$ and 238 $[M-2Me-2d+4H]^+$ ($d \equiv C_4H_7$, see Figure 9) in the EIMS also supported the characterization of **5**.

The NOESY experiment of **5** showed cross peaks as shown in the 3D drawing (Figure 10). The relative configurations at C-2, C-4, and C-6 were deduced from the NOESY cross peaks of H_β-15/H_β-5, H_β-5/Me-13, Me-8/H_β-10, and Me-23/Me-8, which also indicated that the moieties **a–c** were all on the β side.

Based on the information from the ^1H NMR, COSY, and NOESY spectra, a computer-generated 3D structure was obtained by using the above-mentioned molecular modeling program with MM2 force-field calculations for energy minimization. The calculated distances between H_β-15/H_β-5 (2.195 Å), H_β-5/Me-13 (2.782 Å), Me-8/H_β-10 (3.828 Å), and Me-23/Me-8 (2.348 Å) are all less than 4.00 Å; this is consistent with the well-defined NOESY observed for each of the proton pairs. Thus, garcinielliptone J (**5**) was characterized as 7,7-dimethyl-2,6-di(γ,γ-dimethylallyl)-4-(1-oxo-2-methylpropyl)-1,2,3,4-tetrahydrofurano[1,4-*af*]cyclohexa-1,3-dione.

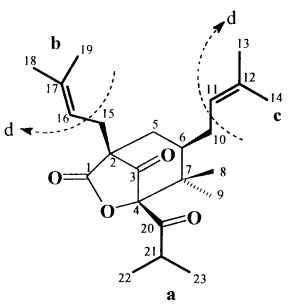

Figure 9. Structure, substructure (bold lines), and MS fragmentation pattern of **5**.

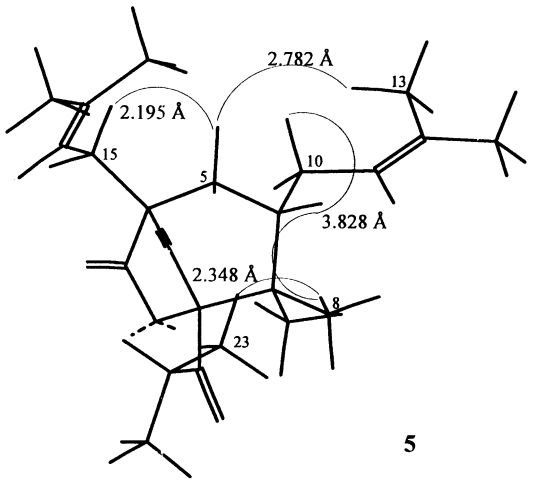

Figure 10. Selected NOESY correlations and relative configuration of **5**.

The anti-inflammatory activities of **1–5** were studied in vitro by measuring their inhibitory effects on chemical-mediator release from mast cells, neutrophils, macrophages, and microglial cells. Compounds **1–5** did not cause a significant inhibition of mast-cell degranulation stimulated with compound 48/80 (10 $\mu g\,mL^{-1}$) (data not shown). Garsubellin A (**7**) (Figure 11) showed a potent inhibitory effect on the release of β-glucuronidase from peritoneal mast cells stimulated with compound 48/80.[5] Replaceing the furano ring in **7** by a pyrano ring reduced at C-2, C-3, C-23, and C-24 and hydroxylated at C-2, C-3, and C-24 (i.e. **3**) did not enhance the inhibitory effect on the release of chemical-mediator from peritoneal mast cells stimulated with compound 48/80 (data not shown). Mepacrine was used in this experiment as a positive control.

The combination fMLP (1 μM)/CB (5 $\mu g\,mL^{-1}$) stimulated the release of β-glucuronidase and lysozyme from rat neutrophils. Compound **1** showed potent inhibitory effects on the release of β-glucuronidase and lysozyme from rat neutrophils stimulated with fMLP (1 μM)/CB (5 $\mu g\,mL^{-1}$). This was carried out in a concentration-dependent manner with IC_{50} values of 26.9 ± 2.6 and 20.0 ± 1.3 μM, respectively, while **2–5** had no significant inhibitory effects (Table 3).

The combination fMLP (0.3 μM)/CB (5 $\mu g\,mL^{-1}$) or phorbol myristate acetate (PMA) (3 nM) stimulated superoxide anion generation in rat neutrophils. As shown in Table 4,

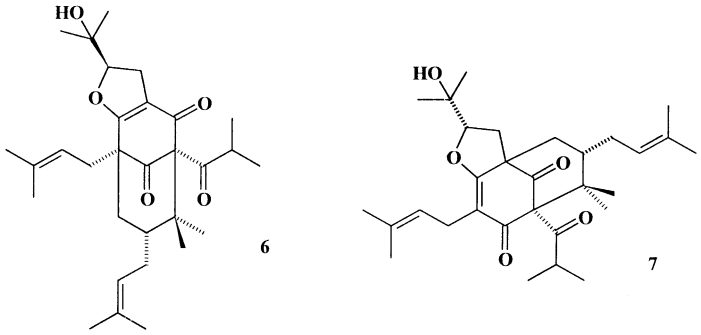

Figure 11. Structures **6** and **7**.

Table 3. The inhibitory effects of **1–5** on the release of β-glucuronidase and lysozyme from rat neutrophils stimulated with fMLP (1 μM)/CB (5 μg mL^{-1}).

Compound	IC_{50} [μM][a] β-Glucuronidase	Lysozyme
1	26.9 ± 2.6	20.0 ± 1.3
2	> 30 (9.0 ± 4.4)	> 30 (6.6 ± 8.9)
3	> 10 (16.8 ± 5.5)	> 10 (−16.0 ± 11.3)
4	> 30 (15.6 ± 2.7)	> 30 (−1.6 ± 7.3)
5	> 30 (0.3 ± 2.3)	> 30 (−24.8 ± 10.2)
trifluoperazine	10.6 ± 0.9	13.2 ± 0.7

[a] When 50% inhibition could not be reached at the highest concentration, the percentage of inhibition is given in parentheses. Data are presented as means ± s.e.m. (n = 3–5). Trifluoperazine was used as a positive control.

Table 4. The inhibitory effects of **1–5** on the superoxide anion generation in rat neutrophils stimulated with fMLP (0.3 μM)/CB (5 μg mL^{-1}) or PMA (3 nM).

Compound	IC_{50} [μM][a] fMLP/CB	PMA
1	17.0 ± 0.9	> 30 (46.8 ± 4.5)
2	> 30 (43.2 ± 3.1)	> 30 (−85.2 ± 6.8)
3	> 3 (−29.2 ± 7.8)	> 3 (−82.5 ± 1.0)
4	> 30 (2.8 ± 5.7)	> 30 (−76.3 ± 7.3)
5	> 3 (23.0 ± 6.0)	> 3 (−24.2 ± 3.4)
trifluoperazine	6.6 ± 0.2	2.7 ± 0.6

[a] When 50% inhibition could not be reached at the highest concentration, the percentage of inhibition is given in parentheses. Data are presented as means ± s.e.m. (n = 3–5). Trifluoperazine was used as a positive control.

compound **1** had a potent inhibitory effect on fMLP/CB-induced superoxide anion generation in rat neutrophils in a concentration-dependent manner with an IC_{50} value of 17.0 ± 0.9 μM, while **2–5** had no significant effect. The above results indicate that cleavage of the furano ring of **6** might enhance its inhibitory effects on fMLP/CB-induced β-glucuronidase and lysozyme release and superoxide anion generation in rat neutrophils.[5] The observation that compounds **1–5** had no appreciable effect on PMA-induced response suggests the involvement of a PMA-independent signaling pathway.[10] Trifluoperazine was used in this experiment as a positive control.

Treatment of RAW 264.7 macrophage-like cells with LPS (1 μg mL^{-1}) or N9 microglial cells with LPS (10 ng mL^{-1})/IFN-γ (10 U mL^{-1}) for 24 h induced NO production. This was assessed by measuring the accumulation of nitrite, a stable metabolite of NO, in the media, based on the Griess reaction. As shown in Table 5, the production of NO induced by LPS/IFN-γ in N9 cells was suppressed in a concentration dependent manner by **4** with an IC_{50} value of 7.4 ± 0.2 μM, while **1–3** and **5** did not show significant effects on the production of NO induced by LPS in RAW 264.7 cells or on NO induced by LPS/IFN-γ in N9 cells. Garsubellin D (**6**) (Figure 11) did show a significant effect on the production of NO in RAW 264.7 cells induced by LPS or in N9 cells induced by LPS/IFN-γ (data not shown). As shown in Table 5, replacing the 1-oxopropyl group of **6** with a benzoyl group (i.e. **4**) might enhance the inhibitiory effect on LPS/IFN-γ-induced NO production in N9 cells. It also indicated that an increase in the lipophilicity of **6** significantly enhanced the inhibitory effects on NO production induced by LPS/IFN-γ in N9 cells. 1400 W was used in this experiment as a positive control.

Table 5. The inhibitory effects of **1–5** on the accumulation of NO_2^- in the culture media of RAW 264.7 cells in response to LPS (1 μg mL^{-1}) and N9 cells in response to LPS (10 ng mL^{-1})/IFN-γ (10 U mL^{-1}).

Compound	IC_{50} [μM][a] RAW 264.7 cells	N9 cells
1	> 10 (22.9 ± 2.9)	> 3 (31.2 ± 0.7)
2	> 3 (30.3 ± 1.0)	> 1 (46.7 ± 0.8)
3	> 10 (15.2 ± 0.5)	> 3 (7.8 ± 5.6)
4	> 30 (17.4 ± 1.5)	7.4 ± 0.2
5	> 30 (−7.7 ± 2.0)	> 30 (5.6 ± 1.5)
1400W[b]	3.0 ± 0.2	2.2 ± 0.1

[a] When 50% inhibition could not be reached at the highest concentration, the percentage of inhibition is given in parentheses. Data are presented as means ± s.e.m. (n = 3–5). [b] *N*-(3-Aminomethyl)benzylacetamidine (1400 W)

The present study suggests that **1** may be valuable in the therapeutic treatment or prevention of peripheral diseases associated with the release of β-glucuronidase, lysozyme, and superoxide anion from neutrophils. The inhibition of NO production by **4** in microglial cells may be of value in the therapeutic treatment or prevention of certain central as well as peripherial inflammatory diseases associated with the increase of NO production.

Further study will be required to clarify the mechanism of action of **1** and **4**.

Experimental Section

General: Optical rotations: JASCO model DIP-370 digital polarimeter. UV Spectra: JASCO UV-VIS Spectrophotometer; λ_{max} (log ε) in nm. IR spectra: Hitachi 260-30 Spectrophotometer; $\tilde{\nu}$ in cm^{-1}. ^{1}H and ^{13}C NMR spectra: Varian Unity-400 spectrometer; 400 and 100 MHz, respectively; δ in ppm, J in Hz. MS: JMS-HX100 mass spectrometer; m/z (rel. %)

Plant material: The fruits of *G. subelliptica* were collected at Kaohsiung, Taiwan, during July 2001. A sample specimen (2003) has been deposited at the Department of Medicinal Chemistry, School of Pharmacy, Kaohsiung Medical University.

Extraction and isolation: The fresh seeds (7.5 kg) obtained from the fresh fruits (22.8 kg) of *G. subelliptica* were extracted with chloroform at room temperature. The $CHCl_3$ extract was concentrated under reduced pressure to afford a brown residue (130 g). This residue was subjected to column chromatography (silica gel). Elution with *n*-hexane/$CHCl_3$ (3:2) yielded **1** (12 mg). Elution with *n*-hexane/acetone (12:1) yielded **2** (10 mg). Elution with $CHCl_3$/ethyl acetate (9:1) yielded **3** (16 mg) and **5** (18 mg). Elution with $CHCl_3$/acetone (9:1) yielded **4** (14 mg).

Garcinielliptone F (1): colorless oil; $[\alpha]_D^{25} = -23°$ (c = 0.09 in $CHCl_3$); ^{1}H NMR ([D_1]$CHCl_3$) and ^{13}C NMR: see Table 1; IR (film on NaCl): $\tilde{\nu}$ = 3439 (OH), 1724 (C=O), 1639 cm^{-1}; UV (MeOH) λ_{max} (log ε): 265 nm (4.07); CIMS: m/z (%): 530 $[M-2+3NH_3-3H]^-$ (4), 514 $[M-2+2NH_3-2H]^-$ (32), 498 $[M-2+NH_3-H]^-$ (35), 483 $[M-1]^-$ (25), 482 (72), 466 (100), 454 (4), 424 (5).

Garcinielliptone G (2): colorless oil; $[\alpha]_D^{25} = -53°$ (c = 0.14 in $CHCl_3$); ^{1}H NMR ([D_1]$CHCl_3$) and ^{13}C NMR: see Table 1; IR (film on NaCl): $\tilde{\nu}$ = 3454 (OH), 1767, 1727, 1708 (C=O), 1665, 1451 cm^{-1}; UV (MeOH) λ_{max} (log ε): 222 nm (4.18); EIMS: m/z (%): 498 $[M-2]^+$ (6), 482 (10), 414 (33), 343 (100), 287 (44); HR-EIMS: calcd for $C_{30}H_{42}O_6^+$ 498.2981; found: 498.2996 $[M-2]^+$.

Garcinielliptone H (3): colorless oil; $[\alpha]_D^{25} = -143°$ ($c = 0.12$ in $CHCl_3$); ^1H NMR ($[D_1]CHCl_3$) and ^{13}C NMR: see Table 2; IR (film on NaCl): $\tilde{\nu} =$ 3439 (OH), 1731, 1712, 1694 (C=O), 1469, 1447 cm^{-1}; UV (MeOH) λ_{max} ($\log\varepsilon$): 210 nm (3.95); EIMS: *m/z* (%): 519 $[M-H_2O+H]^+$ (3), 461 (4), 448 (30), 422 (36), 144 (100); HR-EIMS: calcd for $C_{30}H_{46}O_7^+$ 518.3243; found: 518.3251 $[M-H_2O]^+$.

Garcinielliptone I (4): pale yellow oil; $[\alpha]_D^{25} = +57°$ ($c = 0.20$ in $CHCl_3$); ^1H NMR ($[D_1]CHCl_3$): $\delta = 1.13$ (s, H_3-10), 1.22 (s, H_3-20), 1.32 (s, H_3-21),1.41 (s, H_3-11), 1.50 (m, H_α-7), 1.58 (s, H_3-16), 1.66 (m, H_β-8), 1.69 (s, H_3-15), 1.69 (s, H_3-25), 1.72 (s, H_3-26), 1.76 (dd, $J = 10.8$, 5.6 Hz, H_α-12), 2.01 (dd, $J = 13.2$, 4.0 Hz, H_β-7), 2.19 (dd, $J = 10.8$, 4.4 Hz, H_β-12), 2.53 (m, H_2-22), 2.93 (dd, $J = 15.2$, 7.2 Hz, H_α-17), 3.05 (dd, $J = 15.2$, 10.4 Hz, H_β-17), 4.85 (dd, $J = 10.4$, 7.2 Hz, H-18), 4.98 (t, $J = 6.8$ Hz, H-13), 5.04 (t, $J = 6.8$ Hz, H-23), 7.25 (m, H-30), 7.25 (m, H-32), 7.40 (m, H-31), 7.55 (m, H-29), 7.55 (m, H-33); ^{13}C NMR: 15.9 (C-10), 18.0 (C-16), 18.2 (C-26), 23.1 (C-20), 23.7 (C-11), 26.0 (C-15), 26.0 (C-21), 26.0 (C-25), 27.0 (C-12), 27.1 (C-17), 29.0 (C-22), 39.7 (C-7), 43.3 (C-8), 47.7 (C-9), 55.5 (C-2), 71.8 (C-19), 79.0 (C-6), 93.0 (C-18), 118.3 (C-4), 120.4 (C-23), 122.4 (C-13), 128.0 (C-30), 128.0 (C-32), 128.1 (C-29), 128.1 (C-33), 132.2 (C-31), 133.5 (C-14), 134.8 (C-24), 136.6 (C-28), 175.6 (C-3), 187.7 (C-5), 193.2 (C-27), 206.5 (C-1); IR (film on NaCl): $\tilde{\nu} = 3470$ (OH), 1720 (C=O), 1694, 1620, 1444 cm^{-1}; UV (MeOH) λ_{max} ($\log\varepsilon$): 280 nm (4.11); EIMS: *m/z* (%): 518 $[M]^+$ (7), 450 (18), 435 (10), 381 (55), 345 (5), 327 (53), 105 (100); HR-EIMS: calcd 518.3032 for $C_{33}H_{42}O_5^+$; found: 518.3036 $[M]^+$.

Garcinielliptone J (5): colorless oil; $[\alpha]_D^{25} = -166°$ ($c = 0.18$ in $CHCl_3$); ^1H NMR ($[D_1]CHCl_3$) and ^{13}C NMR: see Table 2; IR (film on NaCl): $\tilde{\nu} =$ 1801 (γ-lactone ring), 1764, 1712 (C=O), 1454 cm^{-1}; UV (MeOH) λ_{max} ($\log\varepsilon$): 210 nm (3.75); EIMS: *m/z* (%): 374 $[M]^+$ (46), 356 (7), 306 (100), 287 (15), 238 (48); HR-EIMS: calcd. for $C_{23}H_{34}O_4^+$ 374.2457; found: 374.2459 $[M]^+$.

Inhibitory assays for chemical-mediator induced by various stimulants in mast cells, neutrophils, RAW 264.7 cells, and N9 cells were performed by the methods described in ref. [11].

Acknowledgement

This work was partially supported by a grant from the National Science Council of the Republic of China (NSC 90-2320-B 037-042).

[1] M. Iinuma, H. Tosa, T. Tanaka, R. Shimano, F. Asai, S. Yonemori, *Phytochemistry* **1994**, *35*, 1355–1360.
[2] H. Minami, M. Kinoshita, Y. Fukuyama, M. Kodama, T. Yoshizawa, M. Sugiura, K. Nakagaw, H. Tago, *Phytochemistry* **1994**, *36*, 501–506.
[3] C. N. Lin, C. W. Kiang, C. M. Lu, R. R. Wu, K. H. Lee, *Chem. Commun.* **1996**, 1315–1316.
[4] M. I. Chung, H. J. Su, C. N. Lin, *J. Nat. Prod.* **1998**, *61*, 1015–1016.
[5] J. R. Weng, L. T. Tsao, J. P. Wang, C. N. Lin, *Chem. Eur. J.* **2003**, *9*, 1958–1963.
[6] Y. Fukuyama, H. Minami, A. Kuwayama, *Phytochemistry* **1998**, *49*, 853–857.
[7] F. W. Mchafferty, *Interpretation of Mass Spectra*, Benjamin, London, **1973**, p. 113.
[8] M. Matsuhisa, Y. Shikishima, G. Honda, M. Ito, Y. Takeda, H. Shibata, T. Higuti, O. K. Kodzhimatov, O. Ashurmetov, Y. Takaishi, *J. Nat. Prod.* **2002**, *65*, 290–294.
[9] L. J. Bellamy, *The Infra-red Spectra of Complex Molecules*, Wiley, New York, **1964**, p. 186.
[10] A. W. Segal, A. Abo, *Trends Biochem. Sci.* **1993**, *18*, 43–47.
[11] H. H. Ko, L. T. Tsao, K. L. Yu, C. T. Liu, J. P. Wang, C. N. Lin, *Bioorg. Med. Chem.* **2003**, *11*, 105–111.

Received: June 6, 2003 [F5209]

